Math. Model. Nat. Phenom.
Vol. 12, No. 5, 2017, pp. 180–195
DOI: 10.1051/mmnp/201712511

A 2D Computational Model of Lymphedema and of its Management with Compression Device

N.Eymard[1], V.Volpert[1,2,3], I.Quere[4], A. Lajoinie[7], P.Nony[5], C.Cornu[6]

[1] Institut Camille Jordan, UMR 5208 CNRS, University Lyon 1, Villeurbanne, France

[2] INRIA Team Dracula, INRIA Antenne Lyon la Doua, Villeurbanne, France

[3] Institute of numerical mathematics, Russian Academy of Sciences, Moscow, Russian Federation

[4] Université Montpellier I, CHU Saint Eloi, Montpellier, France

[5] CHU Lyon, Service de Pharmacologie Clinique et Essais Thérapeutiques, Lyon, France

[6] Hospices Civils de Lyon, Centre d'Investigation Clinique, INSERM CIC 1407, Lyon, France

[7] CHU Lyon, Service de Pharmacologie Clinique et Essais Thérapeutiques, Lyon, France

Abstract. The purpose of this study is to model a lymphedema following a mastectomy and its management (compression therapy). During surgery for breast cancer, an axillary node dissection can be done and cause damages to the lymphatic system leading to a secondary lymphedema located in upper limb. Limb lymphedema is an incurable disease associated with chronic and progressive limb swelling condition. The main clinical consequence of lymphedema is the limb edema, clinically resulting in pain, discomfort, strength reduction and musculoskeletal complications due to limb excessive heaviness. Some devices for lymphedema (e.g. bandaging and garments) could be more personalized, taking into account both characteristics of compressions and patients. Before the evaluation of these therapeutic strategies in humans, an "in silico" approach could be used to investigate the interest of gradual or intermittent compression testing in virtual patients. For that purpose, we developed a simplified model of the lymph flow through the lymphatic system in a whole upper limb including the corresponding interstitial fluid exchanges.

Keywords and phrases: lymphedema, mathematical modeling, compressive device

Mathematics Subject Classification: 35Q30, 35Q35, 35Q68

1. Introduction

Lymphedema can be primary or secondary [1]. The primary lymphedema is a rare, inherited condition caused by problems with the development of lymph vessels. Secondary lymphedema can be caused by damaged lymph system by cancer surgeries and treatments, cardio-vascular dysfunctions and increasingly a result of obesity [1]. Breast cancer-related lymphedema (BCRL), resulting from lymphatic system damage secondary to cancer surgery or radiotherapy, is an important cause of morbidity after breast cancer therapy. Moreover, the onset and the severity of lymphedema depend on multifactorial causes such as number of lymph nodes removed. In our study, we only simulated secondary lymphedema.

Lymphedema is a relatively frequently occurring disease that affects patients' quality of life. In Ref. [2], 72 studies met the inclusion criteria for the assessment of lymphedema incidence, giving a pooled estimate of 16.6% (with a 95% confidence interval [13.6,20.2]) for the disease incidence. Their estimate [2], was 21.4% ([14.9, 29.8]) when restricted to data from prospective cohort studies (30 studies). Therefore it is important to take into account this consequence in breast cancer.

Limb swelling significantly impacts physical, social and psychological aspects of patients' life, see Refs. [3, 4]. As a result of the limb swelling, skin changes are also frequently associated with lymphedema; they are responsible for higher risk of skin infection (recurrent inflammatory episodes, cellulitis) and skin malignancy complication [5](Stewart-Treves syndrome). However, adapted specific skin cares have shown their efficacy for the prevention of skin complications.

Therefore, the main concern in lymphedema management - and the most challenging - is focused on swelling limitation and limb volume reduction, those being fundamental to improve patients' condition and to limit irreversible histological progress of the disease. The purpose of this work is to improve and to personalize compressive devices using an "in silico" modeling approach. To obtain "in silico" results transferable to humans, a mathematical model will be built to simulate the clinical characteristics of the disease (edema) and its evolution with or without care.

1.1. Management of lymphedema

Damages in lymphatic system responsible for lymphedema explain the relative inefficiency of conventional anti-edematous drugs for reducing limb volume, see Refs. [5, 6]. The recent understanding of complex mechanisms of lymphedema formation as well as clinical experience have led to consider physical compression therapy as the most suitable care for lymphedema. Limb external compression therapy, also known as "Decongestive Lymphedema Therapy" (DLT), is presently the focal point of lymphedema management at any stage of the disease, including as a preventive care, see Refs. [5, 7]. Physiologically, DLT aims to reduce limb volume then to maintain volume decongestion (i) by stimulating the failing lymphatics with the use of compression bandages [8], and (ii) by limiting capillary filtration into the interstitial tissue and increasing lymphatic reabsorption. Lastly, the stimulation of lymphatic system improves lymph drainage through remaining functional lymphatic vessels and collateral lymphatic pathways. In practice, DLT consists in a two-phase long-term treatment, see Refs. [7, 8]. The Intensive Phase I, also named as arm initial decongestion, consists in multi-layered bandage compression, applying layers of strong non-elastic bandages that generate high pressure at limb muscle contraction time and low pressure at muscles relaxation time. The usual Phase I duration varies from one to six weeks. This Intensive Phase I is followed by a necessary Maintenance Phase II, aiming at preserving Phase I results using low-stretch elastic garments; this phase is essential for long-term management of lymphedema. Although DLT has been a routine treatment of lymphedema for many years, there is a lack of evidence on the efficacy of compression therapies, which still remains a proof of concept based on physiological knowledge of lymphedema formation. To date, "good studies comparing different compression methods of lymhedema treatment do not exist"[7]. Although the need for the two distinct treatment phases is well recognised, compression technics, which include compressive short-stretch bandages, garments or intermittent pneumatic compression (IPC) therapy, and their optimal implementing modalities are not well defined. Indeed, many parameters would influence DLT efficacy: (i) compression pressure and pressure gradient, (ii) frequency, location, duration and interval of pressure application, (iii) compression stiffness, (iv) type of medical devices (e.g. ready-made and custom-made sleeves, bandages and Velcro, IPC devices) and (v) combination of compression technics (e.g. sleeves or bandages alone or associated with IPC) [4, 9, 10]. As an example, the International Society of Lymphedema recommends the use of Class II or Class III sleeves pressure for Intensive Phase I, and Class I or Class II for Maintenance Phase II, see Ref. [7]. However, there is no evidence allowing the selection of the most appropriate compression class depending on the lymphedema and the patient characteristics. Finally, the main challenge in lymphedema management concerns the optimal way to perform this complex and multi-stage DLT process. Moreover, considering the high inter-individual variability in lymphedema development and response to

DLT, a second important challenge in lymphedema management is to identify predictive factors of DLT efficacy.

1.2. Models of all or part of lymphatic system

In Ref. [11], the already published models can be classified into two categories: lumped and continuum models, referring respectively to the use of ordinary differential / algebraic equations and partial differential equations. In this review of different approaches of lymphatic system modeling, the first model of the entire lymphatic system is attributed to Reddy [12]. This model is a simplified one-dimensional model of the entire lymphatic network based on the Navier–Stokes equations of fluid mechanics. Other models have been developed, such as Macdonald et al. [13] who refined the lymphangion model of Reddy et al. [14] using a short chain of lymphangions and Bertram et al. [15] who modelled a chain of lymphangions using a lumped approach (with valve resistance varying with the pressure gradient across the valve). Similar lumped approaches have been developed by Quick et al. [16], Venugopal et al. [17] and Drake et al. [18] with a simplified algebraic equation based on the time-varying elastance concept. Whereas the models mentioned above are either lumped or one-dimensional, the model of Rahbar & Moore [19] is a three-dimensional model for a single lymphangion. Swartz et al. [44], present a model where bulk tissue fluid movement can be evaluated in situ and described by a linear biphasic theory which integrates the regulatory function of the lymphatics with the mechanical stresses of the tissue.

As already mentioned for Ref. [11], several models of part or all lymphatic system have been developed. However in addition to lymph and interstitial flows modeling, our model has to mimic the emergence and the development of lymphedema over time due to obstruction/destruction of lymphatic vessels. Moreover the simulation of the therapeutic effect of compression techniques (multilayer bandaging, or pressure garments) could be added to our model. Designing and testing personalized devices require new kind of mathematical modeling able to carry out swelling of tissue and flow of lymph.

2. Mathematical model of the disease and of its management

2.1. Models of elastic porous media

The anatomy of the lymphatic system is very complex and we cannot make a realistic modeling of all the ramifications between lymphatic collectors, vessels and capillaries. For this reason, we simulate the behavior of the lymph involved in the process of edema formation: its accumulation causing an edema or its drainage due to compressive device with a mixture theory-based poroelasticity model. This theory is often used to model different biological tissues that can be seen as porous medium, e.g. in Ref. [20]. This theory is very similar to linear elasticity. A term taking into account the fluid pressure is added to the model.

A porous media consists of an elastic matrix (also designated the skeleton of the domain) containing interconnected fluid saturated pores that act as vessels, pores connection allowing the circulation of lymph. Moreover, the matrix deforms under the effect of liquid pressure reproducing the swelling of the limb. Therefore, this matrix will be used to simulate the consequences of lesions and obstructions of lymphatic system without considering the precise and detailed anatomy of the whole lymph system. The superficial lymphatic system surrounding the upper limb drains 90% of the lymph, so we consider the upper limb as a porous matrix surrounding the muscles and the bones.

The upper limb can be considered as a porous medium characterized by a certain value of the porosity coefficient. Consequently, vessels can be associated with a high coefficient value; conversely muscles and bones as tissues with a coefficient equal to zero. In this model, only bones are taken into account. Tissues containing the interstitial lymph have a coefficient with a medium value. This can be considered as a mapping of lymph vessels in upper limb. The model will allow us to calculate fluid velocity and pressure (canalized lymph and interstitial fluid) and the deformation vector field of the computational domain at different stages of the disease.

Similarly, the fluid exchange through the capillary walls cannot be simulated in a whole limb. Exchange of fluid through intravascular and interstitial areas are mainly modeled by Starling's equation, although other models can be used, see Ref. [21]. In Starling's law, a balance between oncotic and hydrostatic pressure in vessels [22], determines a constant drainage and production of interstitial liquid. The movement of fluid between compartments is given by the equality

$$J = K(P_c - P_i) - \sigma(\pi_c - \pi_i)$$

with J, the net fluid movement between compartments, P_c capillary hydrostatic pressure, π_c capillary oncotic pressure, P_i interstitial hydrostatic pressure and π_i interstitial oncotic pressure. In our model, we consider the behavior (pressure and velocity) of a single fluid. The simulated fluid models the canalized lymph and the interstitial liquid. Its pressure is responsible of changes in the volume of porous media, and the increase or decrease in volume of the media acts on fluid pressure and velocity.

The lymph flow inside the lymph vessels is due to muscle activities, to intrinsic contraction of lymphangions caused by the wave stream of contractile smooth cells (CSM) and to venous return. A passive flow is due to surrounding tissue pressure gradients (blood vessel pulsing). Lymphangions have not been considered and the action and possible interaction of the valves with the vessel diameter have been neglected. Reddy et al. [14] assumed the resistance of the valves to be dependent only on the vessel diameter and imposed the condition that the flow rate is positive in all lymphangions. Given the complexity, even the impossibility to our knowledge, to estimate the ratio of each drainage cause and their intensity, we will summarize all the causes of drainage of the lymph by a force, m corresponding to interaction between tissues and fluids. The most commonly used expression of m in the infiltration through deformable porous media theory [23] is given below. We consider the following model to describe fluid motion in a deformable porous medium [23]:

$$\begin{cases} \phi_s + \phi_l = 1, \phi = \phi_s, \phi_l = 1 - \phi, \ (1) \\ \dfrac{\partial \phi}{\partial t} + \ \mathrm{div}(\phi v_s) = 0, \ (2) \\ -\dfrac{\partial \phi}{\partial t} + \mathrm{div}\ ((1-\phi)v_l) = 0, \ (3) \\ \rho_s \dfrac{\partial(\phi v_s)}{\partial t} + \rho_s \mathrm{div}\ (\phi v_s \otimes v_s) - \mathrm{div}\ T_s = m, \ (4) \\ \rho_l \dfrac{\partial((1-\phi)v_l)}{\partial t} + \rho_l \mathrm{div}\ ((1-\phi)v_l \otimes v_l) - \mathrm{div}\ T_l = -m, \ (5) \\ \text{with } m = (1-\phi)^2 \mu_l k^{-1}(v_l - v_s) + p_l\ \mathrm{grad}\phi, \ (6) \end{cases} \tag{2.1}$$

where v_s and v_l are, respectively, the velocity of the solid and of the fluid part of the mixture and p_l is the fluid pressure. The internal force acting between the components is denoted by m. The values of the coefficients ρ_s and ρ_l depend on the nature of the fluid and of the solid. The permeability of the medium is k, and fluid viscosity is μ_l. Next, T_s and T_l are the stress tensors of the solid and liquid phases.

In the mixture theory, a porous medium consists in solid and liquid components, in proportion respectively equal to ϕ_s and ϕ_l. We assume that the binary mixture of components is saturated $\phi_s + \phi_l = 1$. The value of ϕ_l allows us to take in account the infiltration of liquid in interstitial tissues. It increases during the formation of the edema and decreases during the drainage of the edema. We denote $\phi = \phi_s$ and $\phi_l = 1 - \phi$.

The porosity is $\frac{V_p}{V}$, with V_p pores volume and V total volume. The porosity is given by the expression $1 - \phi$. In order to simplify equations of the model [23], we will consider stationary equations and we will neglect the quadratic terms with respect to the fluid velocity assuming that it is small enough. Thus, we consider the Darcy equation for the flow of lymph in porous media and the elasticity equation for the whole limb. In the following, the computational domain simulating the upper limb is denoted by Ω, and

Γ denotes it boundary. It includes the skin surrounding the limb and a non deformable boundary of the domain γ: the proximal area (the shoulder) and the fingertips. The term "solid" refers to the porous media modelling the soft tissues and the terms "liquid or fluid" refer to interstitial fluid and canalized lymph.

2.2. Model of flow of lymph and interstitial liquid

In what follows we will consider the stationary form of equation (4) of the system (2.1) neglecting the inertial terms: $-\text{div } T_l = -m$, where $T_l = -(1-\phi)p_l I$ and I is the identity matrix. Therefore, we obtain the Darcy equation for the flow in porous media:

$$\left\{\begin{array}{r} (1-\phi)u = -\dfrac{k}{\mu_l}\nabla p_l, \text{ in } \Omega \\ \nabla\cdot((1-\phi)u) = W, \text{in } \Omega \\ \left.\begin{array}{r} \dfrac{\partial p_l}{\partial n_\Gamma} = 0, \text{ in } \Gamma \\ \dfrac{\partial p_l}{\partial n_\gamma} = 0, \text{ in } \gamma_{\text{fingertips}} \\ p_l = C_0, \text{ in } \gamma_{\text{shoulder}} \end{array}\right\} \text{ boundaries conditions} \end{array}\right. \tag{2.2}$$

where $u = (u_1(x,y), u_2(x,y))$ is the velocity vector v_l, W is a source term due to production of the interstitial liquid in the arm, p_l is the pressure, k is the permeability coefficient, μ_l is the viscosity coefficient, C_0 is a constant.

The boundary conditions signify that the boundaries are impermeable for the fluid except the proximal area allowing fluid exchange between the upper limb and the rest of the body. The permeability coefficient $k = k(x,y)$ depends on space coordinates because the medium is anisotropic and because of its dependence on ϕ, the proportion of the solid phase in the limb. For fibrous media, the normalized permeability is given by the expression [24]:

$$\frac{k}{d^2} = \frac{1}{\Psi_{CK}}\frac{(1-\phi)^3}{\phi^2}$$

with $\Psi_{CK} \in [80, 320]$ and d the diameter of the fibers. We used a similar form [25]:

$$k = k_0\frac{(1-\phi)^3}{\phi^2}$$

with k_0 a constant depending on pore's shape factors.

In healthy humans, the interstitial fluid is regulated by a balance between oncotic and hydrostatic pressure in vessels [22]. However, in a disturbed lymphatic system equilibrium cannot be achieved. During the disease, there is always an exceed of lymph and its overproduction is modelled by a source term (W) in the equations.

2.3. Elasticity equations

In the stationary case without the inertial terms, the elasticity equation in (2.1) becomes as follows: $-\text{div } T_s = m$. It is written for the solid part of the tissue. Considered for the whole porous medium, the stress tensor T_s is replaced by the tensor $T = T_s(\Theta) - \alpha p I$ [26]:

$$T_{ij} = 2G(\phi)\epsilon_{ij} + (K(\phi) - \frac{2G(\phi)}{3})\delta_{ij}(\epsilon_{11}+\epsilon_{22}) - \alpha(\phi)\delta_{ij}p,$$

$$e_s = (\epsilon_{ij})_{(i,j)} = \frac{1}{2}(\nabla\Theta + \nabla\Theta^t),$$

where $\Theta = (\Theta_x, \Theta_y) = (X - x, Y - y)$ is the displacement, p the pore pressure (also denoted p_{pore}), α an elastic coefficient for a porous material (ratio of fluid volume gained to volume change of element) and $\delta_{ij} = 1$ if $i = j$, $\delta_{ij} = 0$ if $i \neq j$,

$$K = \frac{E}{3(1-2\nu)}, G = \frac{E}{2(1+\nu)},$$

E is the Young's modulus, ν is Poisson's ratio, $\alpha = 1 - \frac{K}{K_s}$. K is the bulk modulus of the porous media, K_s and K_f are the bulk modulus of the matrix. The pore pressure p and the coefficients relating to media characteristics, G, K and α depend on ϕ and also on the drained and undrained conditions (Subsection 2.3.1).

Linear elasticity equations can be used if displacements are small relative to the size of the domain and if the derivatives of displacements are small relative to 1, which is the case in our work. A commonly used criterion to check these conditions is $|tr(\epsilon)| << 1$. With the values of parameters considered in Section 3.2, we have $|tr(\epsilon)| < 9.10^{-2}$ (notation will be explained in Section 2.3). Furthermore, the velocity of solid is negligible in comparison with the velocity of liquid.

2.3.1. Drained and undrained case

Drained and undrained cases are the limiting cases of slow and fast loading, respectively, [27, 28]. In our model, the loading corresponds to the value of the source term. Under undrained conditions, the fluid accumulates in the porous medium leading to pressure increase. Under the undrained conditions, the pressure remains constant. The undrained case is more relevant to our study since the damage caused by surgery or radiotherapy no longer allow the lymph to be efficiently drained, so that the pressure increases during the tissue growth and deformation [27].

We assume that the proportion of liquid and solid phases depends linearly on the pore pressure,

$$\phi = \phi_0 - \alpha \ \mathrm{div}(\Theta) - \delta p.$$

The expression of the coefficient δ depends on drained and undrained conditions, ϕ_0 is the initial value of ϕ:

$$\phi = \phi_0 - \alpha \ \mathrm{div}(\Theta) - (\frac{\alpha^2}{K_u - K} - \frac{1-\phi_0}{K_f})p.$$

There exist different expressions of the undrained bulk of elasticity K_u. We consider it in the following form Ref. [29]:

$$K_u - K = \frac{\alpha^2 K_s K_f}{(1-\phi_0)K_s + (\alpha - 1 + \phi_0)K_f} \ .$$

Then

$$\phi = \phi_0 - \alpha \ \mathrm{div}(\Theta) - \frac{\alpha - 1 + \phi_0}{K_s} p.$$

In Ref. [26], $p = BP$, with B the Skempton pore pressure coefficient and P the total pressure. Moreover in mixture theory, $p_l = (1-\phi)P$. We obtain $p_l = \frac{1-\phi}{B} p_{pore}$.

2.3.2. Incompressibility conditions

We assume that individual material components are incompressible, $\frac{K}{K_s} << 1$ and $\frac{K}{K_f} << 1$. Following [28], we consider the case $\alpha \approx 1$, $B \approx 1$, $K_u \to \infty$ and a linear dependence between the fluid pressure and the pore pressure, $p_l = (1-\phi)p$ [30]. Furthermore, we assume that the coupling is instantaneous. For this limiting situation, all the parameters adopt their upper bound values [26].

Under these assumptions, we obtain the system of equation:

$$\begin{cases} -\ \text{div}\ T = m \\ \phi = \phi_0 - \alpha\ \text{div}(\Theta) - \dfrac{\alpha - 1 + \phi_0}{K_s} p \\ \text{with } m = (1-\phi)^2 \dfrac{\mu_l}{k} u + p\ \text{grad}\phi \\ \Theta = 0 \text{ in } \gamma_{\text{fingertips}} \text{ and in } \gamma_{\text{shoulder}} \\ T \cdot n = 0 \text{ in } \Gamma \end{cases} \tag{2.3}$$

where T is the stress tensor and n is the outward normal vector.

2.4. Tissue remodelling and disease progression

The damaged lymphatic system, unable to drain efficiently the lymph, induces a prolonged exposition to protein-fluid that causes an increase in production of collagen, fatty and connective tissue [32]. This leads to thickening of the skin and of the subcutaneous tissue of the limb [32]. Moreover during accumulation of fluid, fibrin and other protein complexes form an intricate lattice, facilitating the deposition of collagen that leads to a low hydraulic conductivity of tissues [33]. We have to take into account two kinds of phenomena: the fluid accumulation and the tissue remodeling that have been explored in [34],[35] (with a primary lymphedema murine model). This process allows us to explain why the lymphedema seems to increase without limitation if it is not treated, as is the case in elephantiasis, while the elasticity of skin and soft tissue suggest that an equilibrium state should be reached.

Aggravation of the disease over time is thus accompanied by some changes in the soft tissue structure. Our approach consists in the construction of a sequence of computational domains characterised by their size, porosity, permeability and elasticity coefficients. In the model, the temporal and continuous evolution of the upper limb during the disease and its management is replaced by a set of discrete states. The i-th element of this sequence of domains is denoted as "i-th computational domain". It corresponds to a certain step in the tissue remodelling and, consequently, in the progression of the disease and of its treatment.

The deformation of the domain is determined by the equilibrium of fluid pressure and elastic forces. The deformed domain obtained as a result of the simulation at the i-th step is considered as an initial domain at the next step. This means that the elastic forces appeared at the i-th step disappear at the beginning of the (i+1)-step. Biologically, this force relaxation occurs due to the tissue remodelling: tissue fibers become longer under the constantly applied force.

2.5. Mathematical expression of the whole simplified model

Taking into account all hypothesis and simplifications discussed above, we obtain the following model:

– Equation for the pressure, p:

$$\frac{\partial p_l}{\partial x_j} = -(1-\phi_i)\frac{\mu_l}{k} u_j,\ \text{j} = 1,\ 2$$

– Equation for the deformation vector field, T:

$$-\ \text{div}\ T = (1-\phi_i)^2 \frac{\mu_l}{k} u_j + p\ \text{grad}\phi_i,\ \text{j} = 1,\ 2$$

with

$$T_{ij} = 2G(\phi)\epsilon_{ij} + (K(\phi) - \frac{2G(\phi)}{3})\delta_{ij}(\epsilon_{11} + \epsilon_{22}) - \alpha(\phi)\delta_{ij}p$$

and

$$\epsilon_{ij} = \frac{1}{2}(\text{grad}\Theta + \text{grad}\Theta^t)\ \text{i} = 1,\ 2 \text{ and j} = 1,\ 2$$

– $\phi_{i+1} = \phi_i - \alpha(\frac{\partial\theta_1}{\partial x_1} + \frac{\partial\theta_2}{\partial x_2}) - (\alpha - 1 + \phi_i)\frac{p}{K_S(1-\phi_i)}$, $i \in N$

where $k = k_0\frac{(1-\phi_i)^3}{\phi_i^2}$, $E = E_0 e^{a(1-\phi_i)}$, $K = \frac{E}{3(1-2\sigma)}$, $K_S = \frac{E}{3(1-2\sigma_S)}$, $G = \frac{E}{2(1+\sigma)}$, $\alpha = 1 - \frac{K}{KS}$.

At each step of the iterative process, we solve the equations of the model and we recalculate the set of parameters until the area of the limb reaches 1.3 of the initial area. For larger deformations the model may not be applicable.

2.6. Fibrosis

During early stage of the disease (stage one, with an increase of volume less than 20% and without fibrosis), the tissue is still much like normal tissue but it is saturated with liquid. At stage two (with an increase between 20% and 40% and appearance of fibrotic tissues), the swelling extends, and the tissue becomes less responsive to the decongestive therapy. At stage three, the increase in volume is more than 40% and involves other mechanisms that are not considered in this study, in particular, the development of fibrosis in tissues. In this work, we focus on first and second stages of the disease. We can assume that this kind of process results in a rearrangement of the liquid and of the fibrous skeleton in the limb and we also can suppose that the elasticity properties are modified.

Fibrosis spreads in more advanced stages of the disease. We consider that its development only affects the liquid/solid ratio:

$$\phi = W_s + \phi_0 - \alpha\ \mathrm{div}(\Theta) - \frac{\alpha - 1 + \phi_0}{K_s}p,$$

where W_s is a constant.

With an early management of lymphedema and before an important development of fibrosis, we assume that the changes in the tissue are reversible. Therefore, the original form of the upper limb can be obtained after the compression.

2.7. Model of the compressive device

The mathematical model developed in this work allows us to test the compression device and to vary the value of the applied compression force and the location of its application. Several types of bandaging or garments are available. They are ranked in order of the pressure range. The values for each class are given on an indicative basis because they are chosen by the producers. We consider class 1: 18–21 mmHg, class 2: 23–32 mmHg, class 3: 34–46 mmHg, class 4: $\geq$49 mmHg. The application of the compression forces and the reduction of edema can be modeled by a new boundary condition in the elasticity equation (2.3): $T \cdot n = F$ instead of $T \cdot n = 0$ at the deformable boundaries of the domain, where F is the normal force due to bandage. In general, it depends on the space coordinates.

3. Implementation of the model

3.1. Variational and computational forms of equations

We consider the Darcy equations (2.2) to model the lymph flow and the elasticity equations (2.3) to determine the deformation of the medium. The computational domain has a complex geometry, and it changes during the disease development and treatment. The implementation of the model is done with the solver FreeFem^{++} ([37]) and OS Ubuntu.

The equations of fluid motion are considered in the variational form:

$$\int_\Omega \frac{k}{\mu_l}\nabla p \cdot \nabla q - \int_\Omega Wq = 0. \tag{3.1}$$

Here q is a test function.

Using Green's formula and the boundary conditions, we obtain the variational form of the elasticity equations:

$$\int_\Omega (2G\epsilon_{ij}(\Theta) : \epsilon_{ij}(\Psi) + (K - \frac{2G}{3})\nabla \cdot \Theta \nabla \cdot \Psi - \alpha p \nabla \cdot \Psi) - \int_\Omega m\Psi = 0, \tag{3.2}$$

where Ψ is a test function. Equations (3.1) and (3.2) are implemented in the software.

The computational domain is limited by three types of boundaries: fixed permeable boundary with the shoulder and fingertips, deformable impermeable boundary representing the skin surrounding the limb, fixed impermeable boundary between the soft tissue and the bone inside it (Figure 1).

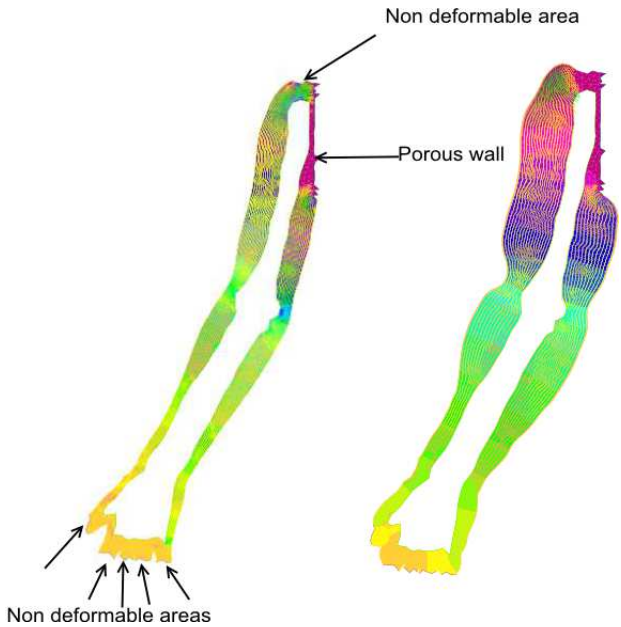

FIGURE 1. Visualisation of the solution of the equations (3.1) with the finite element method implemented in the solver FreeFem^{++}. We used the default view with the drawing of isovalues of real FE–functions (the pressure of the fluid, p) shown with the gradient of color and of the vector field shown by the arrows (the velocity of the fluid $u = (u_1(x, y), u_2(x, y))$. The displacement vector field ($\Theta = (\Theta_x, \Theta_y)$, equation (3.2)) is applied to each point of the initial computational domain and determines its deformation. Under the fluid pressure, the geometry of the domain can change.

3.2. Calibration of the model

An upper limb of the virtual patient is defined by a set of parameters which determine the elasticity and porosity of the biological tissues and of the flow. The values of some parameters are unknown, including the constant k_0 in the expression of permeability and the value C_0 of the pressure at the boundary with the shoulder. In this case, their values are fitted to obtain known values of the pressure and of the flow velocity in the limb.

3.2.1. Source term

The value of W determines the severity of damage in the lymphatic system. Though the source term W can depends on the space coordinate, for the sake of simplicity we suppose that it is constant, $W(x, y) =$

w_0. Figure 2 shows the change of volume of the upper limb during the disease development. As it can be expected, it increases faster for larger values of W.

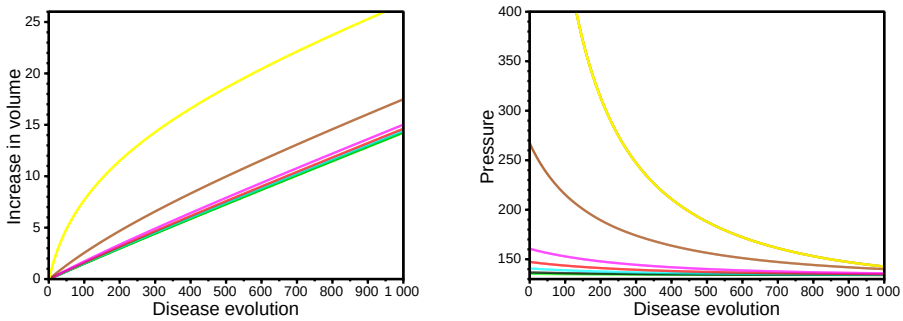

FIGURE 2. Numerical simulation for fixed value $C_0 = 134$ Pa of pressure at the boundary. Left: percentage of volume increase in the upper limb. Right: median fluid pressure inside the upper limb. The results are obtained for $W = 10^{-7}$ kg.m^2 (green), $W = 2.10^{-7}$ kg.m^2 (black), $W = 5.10^{-7}$ kg.m^2 (blue), $W = 10^{-6}$ kg.m^2 (red), $W = 2.10^{-6}$ kg.m^2 (purple), $W = 10^{-5}$ kg.m^2 (brown), $W = 10^{-4}$ kg.m^2 (yellow).

3.2.2. Pressure and boundaries conditions

The study [38] shows that the pressure in the upper limb with lymphedema is in the range between -1.5 and 10 mmHg. The median of maximum pressure generated by the lymphatic pump is 39 ± 14 mmHg for healthy subjects [39]. It is 22.50 ± 18.3 mmHg in the dominant arm (right or left) and 25 ± 20 mmHg in the non-dominant arm [40]. The lymphatic circulation depends on the pressure at the boundary.

3.2.3. Permeability

The permeability depends on the porosity and the constant value k_0. Figure 3 shows the impact of k_0 on the results. As it can be expected, for higher values of k_0 the flow velocity increases and the pressure decreases.

3.2.4. Elasticity coefficient

The upper limb represents a very heterogeneous medium composed by different tissues such as bones, skin, blood and lymphatic vessels and muscles. Each of them has its own value of Young's modulus and Poisson's ratio. In particular, the value of E can vary between 10^3 Pa and 10^6 Pa [41–43]. Moreover, they can depend on the porosity. We use an empirical expression for these coefficients given by the Spriggs equation $E = E_0 \exp(-(1-\phi)a)$ [31]. The values of a is specific to the medium, E_0 corresponds to the zero-porosity. We observe larger deformation of the limb for higher values of a (not shown).

3.2.5. Values of parameters

The simulations of this section are performed with $C_0 = 500$ Pa, $k_0 = 10^{-6}$ D, $W = 10^{-4}$ kg.m^2, $a = 2$ and $E_0 = 5.10^5$ Pa, unless otherwise indicated in figure captions. The other values of parameters are given in Table 4. For these values, the pressure inside the upper limb belongs to the expected range and the velocity approaches the observed value in a healthy subject 0.00148 $m.s^{-1}$.

3.3. Simulation of lymphedema

The proportion of fluids in human body is approximately 60% but it differs significantly between different tissues of body and different individuals. All these factors make it difficult to estimate the porosity of

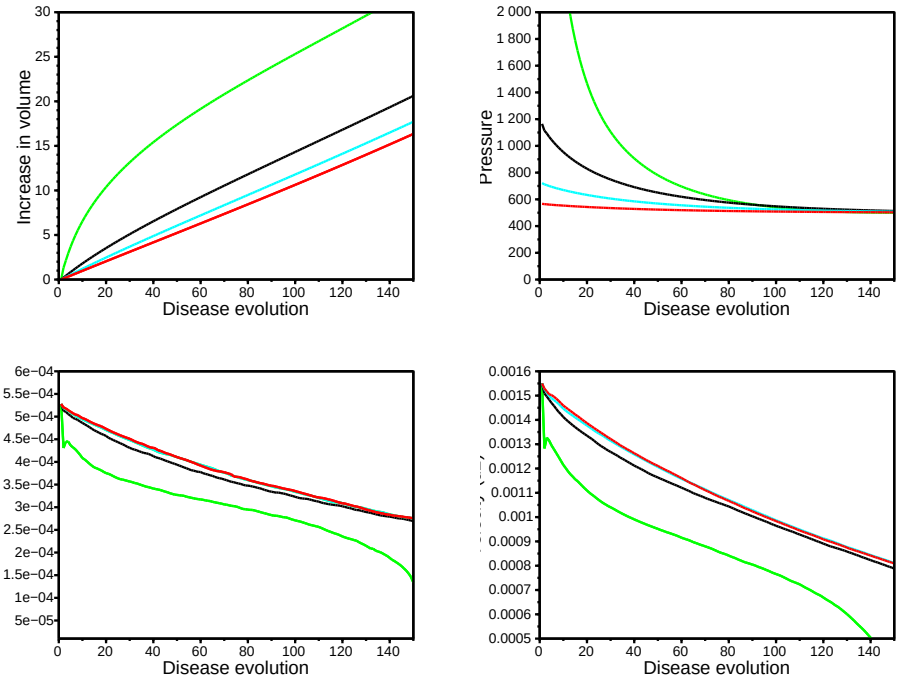

FIGURE 3. Numerical simulations for the fixed values $W = 5.10^{-6}$ kg.m^2 and $C_0 = 500Pa$. The results are obtained for $k_0 = 10^{-7}$ D (green), $k_0 = 10^{-6}$ D (black), $k_0 = 5.10^{-6}$ D (blue), $k_0 = 10^{-5}$ D (red). (a) percentage of volume increase in the upper limb, (b) fluid pressure variation, (c) and (d) show the the components of the flow field $u_1(x, y)$ and $u_2(x, y)$, respectively.

the upper limb. In our model, we consider $\phi \in [\phi_{min}, \phi_{max}]$ with $\phi_{min} = 0.01$ and $\phi_{max} = 0.99$. In the following simulations, the initial value of ϕ is supposed to be constant (space independent), $\phi(x, y) = \phi_0$.

3.3.1. Simulation of compressive device

We apply the force $F = F(x_1, x_2)$ to the outer boundary Γ of the domain (skin of the patient). In the 2D model, it is a one-dimensional curve. We set $P = \frac{F}{S}$ and $P = f$, with F a normal force. We take into account two phases of treatment. The acute phase begins when the increase in the volume due to the edema exceeds a given value (20% in Figure 4). The maintenance treatment begins when the edema is reabsorbed in order to prevent a new edema. The difference between the treatment of these two stages is the maximum value of the applied pressure to stress. A lower pressure to stress is sufficient to keep the volume constant when the edema is not present.

3.3.2. Acute phase

We consider three different compression forces:

– constant: a constant force is applied on the upper limb,

$$f(y) = f_0, \tag{3.3}$$

– decreasing: the force decreases linearly toward the wrist,

$$f(y) = f_\alpha \frac{y - y_{min}}{y_{max} - y_{min}}\ , \tag{3.4}$$

– increasing: the force increases linearly toward the wrist,

$$f(y) = f_\alpha \frac{y_{max} - y}{y_{max} - y_{min}} \ . \tag{3.5}$$

In the last two cases, we will denote the mean value of the force by $f_0 (= f_\alpha/2)$. As we can expect, the efficiency of the compression device increases together with the applied force (Figure 4 (right)).

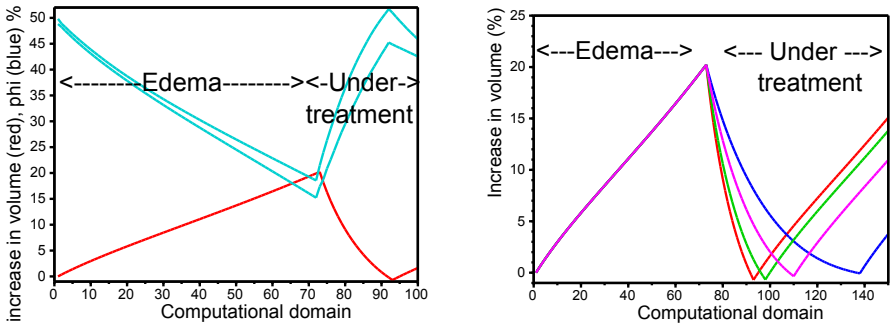

FIGURE 4. Simulation of lymphedema with the parameters from Table 1 and a constant compression force. After 20% of volume increase the compression device is applied. Left: volume change for $f_0 = 4667$ Pa (35 mmHg) (red), minimal and maximal values of ϕ (blue). Right: volume change for $f_0 = 4667$ Pa (35 mmHg) compression class 3 (red), $f_0 = 4000$ Pa (30 mmHg) compression class 2 (green), $f_0 = 3067$ Pa (23 mmHg) compression class 2 (purple). $f_0 = 2333.5$ Pa (17.5 mmHg) compression class 1 (blue).

3.3.3. Comparison between different forces

The standard practice is to applied higher force at the wrist and less force at the shoulder. In Figure 5, we compare three different distributions of applied forces with the same mean value. The volume of the limb decreases faster for the force (3.4) decreasing from the shoulder to the wrist. From this point of view, this is the best force distribution; which is contrary to usual practices based on the assumption that an external compression of the extremity needs to be graduated or "degressive". Clinical trial with distally decreasing pressure (called an inverse gradient pressure) on patients with advanced venous insufficiency has been carried out by Mosti and Partsch [36]. Our results are relevant with the conclusion of their study, in which they obtain best results with an inverse gradient pressure. The intermediate one is obtain for the constant force (3.3) and the worst for (3.5).

3.3.4. Maintenance phase

Since the lymphatic system is damaged, the overproduction of lymph still exists after the acute phase and the edema develops again if the device is removed. We simulate different modalities of devices during the maintenance phase (not shown). After the decongestion obtained with care in the acute phase, a new edema occurs. When the cumulative increase of volume exceeds 5%, the maintenance care begins. With simulations, we observe a stabilisation of the volume during the maintenance phase for lower values of compression forces than for the acute phase.

4. Discussion and perspectives

There are different approaches to model the lymphatic system [11]. The goal of this work is to model the whole upper limb. Therefore, we cannot consider individual vessels and we use a macroscopic approach

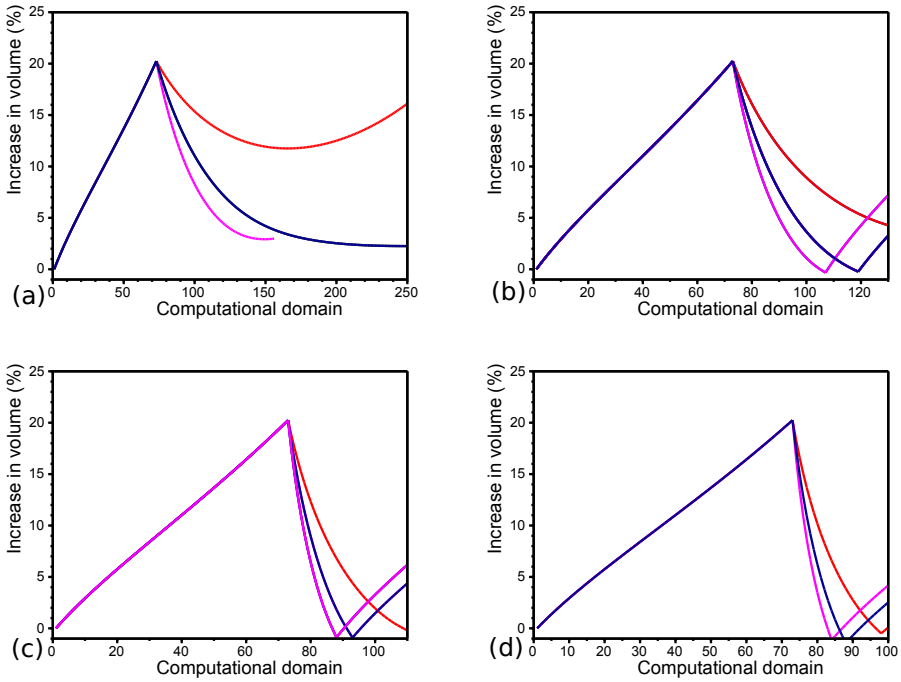

FIGURE 5. Simulation of lymphedema with the parameters from Table 1 and different compression forces with the same mean value. The force (pressure) increases linearly toward the wrist, (3.5) (red), constant value, (3.3) (blue), the force decreases linearly toward the wrist, (3.4) (purple). (a) mean value of pressure: 1500 Pa (11 mmHg), (b) mean value of pressure: 2667 Pa (20 mmHg), (c) mean value of pressure: 4667 Pa (35 mmHg), (d) mean value of pressure: 6000 Pa (45 mmHg).

where the limb tissue is modeled as an elastic porous medium with a lymph flow described by the Darcy equation. In the case of lymphedema, lymphatic system is damaged resulting in the development of edema. This model allows us to test the efficiency of treatment depending on the compression intensity and on the force application area. We show that the force increasing from the wrist to the shoulder is more efficient than a constant or a decreasing force.

This modelling approach has some limitations. In particular, the constitutive relations for the biological tissues are empirical and they should be tested experimentally in more detail. Furthermore, the biophysical properties of the tissues (elasticity, porosity) are not well known. Finally, this medium is highly heterogeneous, and we need to use various approximations and simplifications.

Such a disease modeling approach may contribute to the generation of new hypotheses for alternative therapeutic strategies that could be further tested in a more global framework. In this study, we did not consider all the different modalities of compressive garments such as stiffness or interval of pressure application. We focused on the compression pressure and pressure gradient.

Thus, in silico' RCTs modeling and simulation performed in different specific virtual populations of patients can be helpful to delineate the optimal trial design/patients' characteristics to consider in terms of time duration of the trial, number of needed patients and precision of the estimation of treatment effects. However, such a global "in silico" approach will always require a final and consistent validation using corresponding in vivo clinical trials carried out in real patients. The choice of the most efficient

treatment depending on the individual patient characteristics (age, sex, mass body index) will require further investigations.

Moreover, it is known that the compression of the bandaging can depend on the person (physician, nurses,...) that provide them. According to a study including 891 health care professional, Protz et Al. [45] concluded to a lack of knowledge of the majority of them. Even in case of garments with technical specifications, the pressure to stress can vary. Indeed, the fabric of the garment can relax with time or can be misused by the patient. Our "In silico approach" did not take into account these sources of variation but in future clinical trials, they must not be underestimated. They are responsible of a large variability in the efficiency of the treatment.

Acknowledgements. The work was partially supported by Russian Science Foundation (Grant no. 15-11-00029).

References

[1] M. Benson, R. Gaskin, C. Moffatt, V. Peach, M. Mitchell, C. Faull. *P-86 developing and implementing a community care pathway for the management of chronic oedema.* BMJ Supportive & Palliative Care, 6 (Suppl 1):A41–A41, 2016

[2] T. DiSipio, S. Rye, B. Newman, S. Hayes. *Incidence of unilateral arm lymphedema after breast cancer: a systematic review and meta-analysis* Lancet Oncology, vol. 14, no. 6 (2013), 500-15.

[3] M.B. Tobin, H.J. Lacey, L. Meyer et al. *The psychological morbidity of breast cancer-related arm swelling. Psychological morbidity of lymphedema.* Cancer., 72 (1993), 3248-52.

[4] P.A. Morgan, P.J. Franks, C.J. Moffatt. *Health-related quality of life with lymphedema: a review of the literature.* International wound journal., 2 (2005), 47-625.

[5] P.S. Mortimer, Managing lymphoedema, Clinical and experimental dermatology, 20 (1995), 98-106.

[6] N.B. Piller, R.G. Morgan, J.R. Casley-Smith. *A double-blind, cross-over trial of O-(beta-hydroxyethyl)-rutosides (benzo-pyrones) in the treatment of lymphoedema of the arms and legs.* British journal of plastic surgery; 41 (1988), 20-7.

[7] The diagnosis and treatment of peripheral lymphedema: Consensus Document of the International Society of Lymphology. Lymphology, 46 (2013), 1-11.

[8] H. Partsch, N. Stout, I. Forner-Cordero et al. *Clinical trials needed to evaluate compression therapy in breast cancer related lymphedema (BCRL). Proposals from an expert group.* Int Angiol., 29 (2010), 442-53.

[9] I. Quere, E. Presles, M. Coupe et al. *Prospective multicentre observational study of lymphedema therapy: POLIT study.* Journal des maladies vasculaires, 39 (2014), 256-63.

[10] C.J. Moffatt, P.J. Franks, D. Hardy et al. *A preliminary randomized controlled study to determine the application frequency of a new lymphoedema bandaging system.* The British journal of dermatology, 166 (2012), 624-32.

[11] K.N. Margaris, R.A. Black. *Modelling the lymphatic system: challenges and opportunities.* Published online before print 11 January 2012, J. R. Soc., Interface doi: 10.1098/rsif.2011.0751.

[12] N.P. Reddy. *A discrete model of the lymphatic system.* PhD thesis, Texas A&M University, TX, 1974.

[13] A.J. Macdonald, K.P. Arkill, G.R. Tabor, N.G. McHale, C.P. Winlove. *Modeling flow in collecting lymphatic vessels: one–dimensional flow through a series of contractile elements.* Am. J. Physiol. Heart Circ. Physiol.; 295, H305–H313. (doi:10.1152/ajpheart.00004.2008).

[14] N.P. Reddy, T.A. Krouskop, P.H. Newell. *Computer–model of lymphatic–system.* Comput. Biol. Med., 7 (1977), 181–197. (doi:10.1016/0010-4825(77)900)

[15] C.D. Bertram, C. Macaskill, J.E. Moore. *Simulation of a chain of collapsible contracting lymphangions with progressive valve closure.* J. Biomech. Eng. Trans., ASME 133, 011008, 2011 (doi:10.1115/1.4002799).

[16] C.M. Quick, A.M. Venugopal, R.M. Dongaonkar, G.A. Laine, R.H. Stewart. *First-order approximation for the pressure–flow relationship of spontaneously contracting lymphangions.* Am. J. Physiol. Heart Circ. Physiol., 294, H2144–H2149, 2008. (doi:10.1152/ajpheart.00781.2007)

[17] A.M. Venugopal, R.H. Stewart, G.A. Laine, R.M. Dongaonkar, C.M. Quick. *Lymphangion coordination minimally affects mean flow in lymphatic vessels.* Am. J. Physiol. Heart Circ. Physiol., 293, H1183–H1189, 2007. (doi:10.1152/ajpheart.01340.2006)

[18] R.E. Drake, S.J. Allen, J. Katz, J.C. Gabel, G.A. Laine. *Equivalent–circuit technique for lymph–flow studies.* Am. J. Physiol., 251 (1986), 1090–1094.

[19] E. Rahbar, J.E.J. Moore. *A model of a radially expanding and contracting lymphangion.* J. Biomech., 21 (2011), 118–123.

[20] S.C. Cowin. *Bone poroelasticity.* Journal of Biomechanics, 32 (1999), 217–238.

[21] E. Vicaut. *Mécanismes des échanges d'eau : équations de Starling.* Am. Fr. Anesth. Réanim., 15 (1996), 428–435 [in french].

[22] D.O. Bates, J.R. Levick, P.S. Mortimer. *Starling pressures in the human arm and their alteration in postmastectomy oedema.* Journal of Physiology, vol. 477, issue 2 (1994), 355–363.

[23] D. Ambrosi. *Infiltration through Deformable Porous Media.* Math. Mech., ZAMM Z. Angew. Math. Mech., vol. 82, no. 2 (2002), 115–124.

[24] K. Yadchi, S. Srivastava, S. Luding. *On the validity of the Carman–Kozeny equation in random fibrous media II International Conference on Particle-based Methods– Fundamentals and Applications.* PARTICLES, E. Oñate and D.R.J. Owen (Eds), 2011.

[25] J.I. Siddique, F.A. Landis, M.R. Mohyuddin. *Dynamics of Drainage of Power-Law Liquid into a Deformable Porous Material.* Open Journal of Fluid Dynamics, 4 (2014), 403-414.

[26] E. Detournay, AH-D. Cheng. *Fundamentals of poroelasticity, Chapter 5 in Comprehensive Rock Engineering: Principles, Practice and Projects.* Vol. II, Analysis and Design Method, ed. C. Fairhurst, Pergamon Press, 113-171, 1993.

[27] J.R. Rice. *Elasticy of fluid-infiltrated porous solids. revised list of references.* August 2001 and April 2004) For use in Engineering Science 265, Advanced environmental geomechanics, 1998.

[28] H.F. Wang. *Theory of linear poroelasticity.* Princeton, NJ: Princeton Univ. Press, 2000.

[29] R.C. Nolen-Hoeksema. *Modulus-porosity relations, Gassmann's equations, and the low-frequency elastic-wave response to fluids.* Geophysics, vol. 65, no. 5 (2000) 1355–1363.

[30] K. Wilmanski. *A few remarks on Biot's model and linear acoustics of poroelastic saturated materials.* http://www.mech-wilmanski.de, University of Zielona Gora (Poland)

[31] J.C. Wang. *Young's modulus of porous materials.* Journal of Materials Science, vol. 19, Issue 3 (1984), 801–808.

[32] Medifocus guidebook on : Lymphedema. 2012 Medifocus.com, Inc. Guide OC 030.

[33] J.A. DeLisa, B.M. Gans, N.E. Walsh. *Physical Medicine and Rehabilitation: Principles and Practice*, Volume 1, Lippincott Williams & Wilkins, 2005.

[34] S.G. Rockson. *Acquired Lymphedema: Abnormal Fluid Clearance Engenders Tissue Remodeling.*Lymphat Res Biol., vol. 12, no. 1(2014), 1-1. doi:10.1089/lrb.2014.1211.

[35] J.M. Rutkowski, C.E. Markhus, C.C. Gyenge, K. Alitalo, H. Wiig, M.A. Swartz. *Dermal Collagen and Lipid Deposition Correlate with Tissue Swelling and Hydraulic Conductivity in Murine Primary Lymphedema.* The American Journal of Pathology, vol. 176, no. 3 (2010), 1122-9.

[36] G. Mosti, H. Partsch. *Compression stockings with a negative pressure gradient have a more pronounced effect on venous pumping function than graduated elastic compression stockings.* European Journal of Vascular and Endovascular Surgery, vol. 42, no. 2 (2011), 261–266.

[37] F. Hecht. *New development in FreeFem^{++}*, J. Numer. Math., vol. 20, no. 3-4 (2012), 251–265.

[38] W.L. Olszewski, P. Jain, G. Ambujam, M. Zaleska, M. Cakala, T. Gradalski. *Tissue Fluid Pressure and Flow during Pneumatic Compression in Lymphedema of Lower Limbs.* Lymphatic research and biology, vol. 9, no. 2, 2011.

[39] S. Modi, A.W.B. Stanton, W.E. Svensson, A.M. Peters, P.S. Mortimer, J.R. Levick. *Human lymphatic pumping measured in healthy and lymphoedematous arms by lymphatic congestion lymphoscintigraphy.* J. Physiol. vol. 583, no. 1 (2007), 271–285.

[40] W.L. Olszewski. *The "third" circulation in human limbs tissue fluid, lymph and lymphatics.* www.phlebologieonline.de on 2015-06-26 – IP: 134.214.22.18. Phlebologie, vol. 41, no. 6 (2012), 283-338, 297–303.

[41] WCC. Lee, M. Zhang. *Using computational simulation to aid in the prediction of socket fit : A preliminary study.* Medical Engineering and Physics, vol. 29, no. 8, (2007), 923–929.

[42] A. Zhang, X.Q. Dai, Y. Li, JT-M. Cheung. *Computational simulation of skin and sock pressure distributions.* Studies in Computational Intelligence, 55 (2007), 323–333.

[43] X. Dai, R. Liu, Y. Li, M. Zhang, Y. Kwok. *Numerical simulation of skin pressure distribution applied by graduated compression stockings.* Studies in Computational Intelligence, 55 (2007), 301–309.

[44] M.A. Swartz, A. Kaipainen, P.A. Netti, C. Brekken, Y. Boucher, A.J. Grodzinsky, R.K. Jain. *Mechanics of interstitial-lymphatic fluid transport: theoretical foundation and experimental validation.* Journal of Biomechanics, 32 (1999), 1297–1307.

[45] K. Protz, K. Heyer, M. Dörler, M. Stücker, C. Hampel-Kalthoff, M. Augustin. *Compression therapy: scientifc background and practical applications.* JDDG: Journal der Deutschen Dermatologischen Gesellschaft, vol. 12, no. 9 (2014), 794–801.

Appendix. The values of parameters

TABLE 1. Values of parameters used in simulations unless other values are specified in curve's legends.

Parameter	Value	Unit
W	10^{-6}	kg.m^2
E_0	5×10^6	Pa
C_O	500	Pa
k_0	10^{-6}	Darcy
μ_l	1.4×10^{-3}	Pa.s^{-1}
ϕ_0	50%	-
ϕ_{min}	0%	-
ϕ_{max}	100%	-
ν	0.3 range[0–0.5]	-
a	2	-